JET–P(98)70

M Keilhacker

JET Deuterium-Tritium Results and their Implications

JET–P(98)70

JET Deuterium-Tritium Results and their Implications

M Keilhacker.

JET Joint Undertaking, Abingdon, Oxfordshire, OX14 3EA,

Preprint of a Paper to be published in
Philosophical Transactions of the Royal Society

January 1999

ABSTRACT

During the second half of 1997, JET carried out a broad-based series of experiments in deuterium-tritium (D-T) producing a total of 675 MJ of fusion energy and setting records for fusion power (16 MW), ratio of fusion power to plasma input power (0.62, and 0.95 ± 0.17 if a similar plasma could be obtained in steady-state) and fusion power duration (4 MW for 4 s). A large scale tritium supply and processing plant, the first of its kind, allowed the repeated use of the 20 g tritium on site, supplying a total of 99.3 g of tritium to the machine.

The D-T physics programme allowed the size, heating requirements and operating conditions of the International Thermonuclear Experimental Reactor (ITER) to be defined more precisely. The threshold power required to access the high confinement operating mode foreseen for ITER is significantly lower in D-T than in deuterium (giving increased operational flexibility for ITER) but the global energy confinement time itself is practically unchanged (no isotope effect). ITER demonstration pulses, in which the important dimensionless parameters for confinement were matched to those of ITER, predict ignition for ITER provided the required densities can be reached. Three radio frequency schemes for heating ITER were also tested successfully in D-T. The results agreed well with code calculations giving confidence in the use of these models for predicting ICRF heating in future machines. Finally, the D-T experiments provided the first clear evidence of alpha-particle heating, showing it to be consistent with classical expectations and confirming the process by which ignition and thermonuclear burn will occur in ITER and a fusion reactor.

1. INTRODUCTION

The Joint European Torus (JET) is the only tokamak experiment that was designed from the outset for deuterium-tritium (D-T) operation and uses comprehensive tritium processing and remote handling systems. In 1991, after eight years of operation, JET had achieved a plasma performance in deuterium which, if reproduced in a 50:50 D:T mixture, would have constituted breakeven conditions. It was decided that this performance warranted a Preliminary Tritium Experiment (PTE) to gain experience with D-T mixtures and to validate D-T fusion predictions. To limit the activation of the machine a mixture of only 10% tritium and 90% deuterium was used and only two, practically identical, pulses were carried out. Each pulse produced a peak fusion power of 1.7 MW averaging 1 MW for 2 s and a fusion gain P_{fus}/P_{in}=0.12 [1]. This was the world's first controlled production of significant fusion power.

In 1997 (May to June and September to November), JET resumed D-T operation with a broad-based but closely focused series of D-T experiments (DTE1) which addressed specific questions relating to D-T physics and technology for ITER and a reactor. This paper describes the results from these D-T experiments (see also [2-4]) and discusses their implications for the approach to ignition in general and, more specifically, for the extrapolation to the International

Thermonuclear Experimental Reactor (ITER) [5] defined as the plasma core of a future fusion reactor, i.e. demonstrating ignition and long pulse burn.

JET is unique for providing pertinent results in this area. It is essentially a one-third scale model of ITER, nearest in size and operating conditions to ITER and with a very similar plasma and divertor configuration. In addition, after the completion of TFTR in April 1997, JET is now the only experiment world-wide able to operate with D-T mixtures. JET has also developed a unique capability for remote installation and repair which was used successfully earlier in 1998 for a major modification to its divertor in the activated environment following DTE1.

In the context of the approach to an ignited plasma, the paper addresses four major issues of fusion physics. The first is to define the parameters of a Next Step tokamak and the JET results confirm that the ITER parameters are the right ones for its stated objectives. The second issue is to characterise the standard operating mode for ITER, the ELMy H-mode. Here the JET D-T results allow a more accurate assessment of the ignition margins and heating requirements of ITER. The third issue is to confirm the process by which ignition and burn would occur in ITER and a reactor. The JET results help to validate the high performance physics in D-T and, in particular, provide an unambiguous demonstration of alpha-particle heating. The fourth issue addressed is the optimisation of tokamak operation for ignition and long pulse operation at reduced plasma current (and thereby size and cost) in ITER and a reactor. Here the JET experiments provide the first demonstration in D-T of the control of plasma profiles in such an advanced operating mode, the so-called optimised shear scenario. This discussion of fusion physics issues is complemented by a section on tritium retention where DTE1 has provided valuable information for ITER.

The paper is structured in the following way. Section 2 discusses how the tritium was supplied to the torus and how much of it was retained in the torus after DTE1. Section 3 characterises the standard operating mode for ITER (steady-state ELMy H-mode) in D-T, addressing the isotope effect on the threshold power for high confinement and the energy confinement time itself and making predictions for ITER. Section 4 deals with ion cyclotron resonance frequency heating of ELMy H-mode D-T plasmas. Section 5 addresses D-T performance and related physics, including records in fusion performance, Alfvénic instabilities and alpha particle confinement and heating. Section 6 presents the advanced operating mode for ITER (optimised shear mode) in D-T: the formation of an internal transport barrier with diffusion coefficients reduced to neoclassical values, the co-existence of internal and edge transport barriers and the possible development of this scenario towards steady-state. The summary and conclusions follow in Section 7.

2. TRITIUM SUPPLY, CONCENTRATIONS AND INVENTORY

During DTE1, 20 g of tritium were stored on the JET site in U-beds. This tritium was supplied, collected from the exhaust gases and reprocessed by an industrial scale tritium processing plant which worked in a closed-cycle with the tokamak, pumping the torus in continuous operation. In all, 99.3 g of tritium was supplied to the JET machine, requiring eight processing cycles in which the tritium was routinely separated to better than 99.5% purity. The tritium gas was either injected directly into the torus via a gas valve (a total of 35 g) or by Neutral Beam (NB) injection. In this latter case only a small fraction of the tritium gas supplied to the NB box was injected into the torus via the high energy tritium neutral beams. The remaining tritium gas was trapped by the NB cryopumps and was recovered to better than 98% in nightly regenerations.

One of the experiences of DTE1 was that the tritium concentrations in the plasma could be relatively easily controlled by loading the walls to an appropriate level of tritium using ohmic or low power ICRF heated discharges. As shown in Fig. 1(a), plasma tritium concentrations greater than 90% were readily obtained. Figure 1(a) also shows that during DTE1 and during the ensuing clean-up phase tritium concentrations in the plasma and exhaust gases were reduced at a rate similar to the experience from the PTE [6].

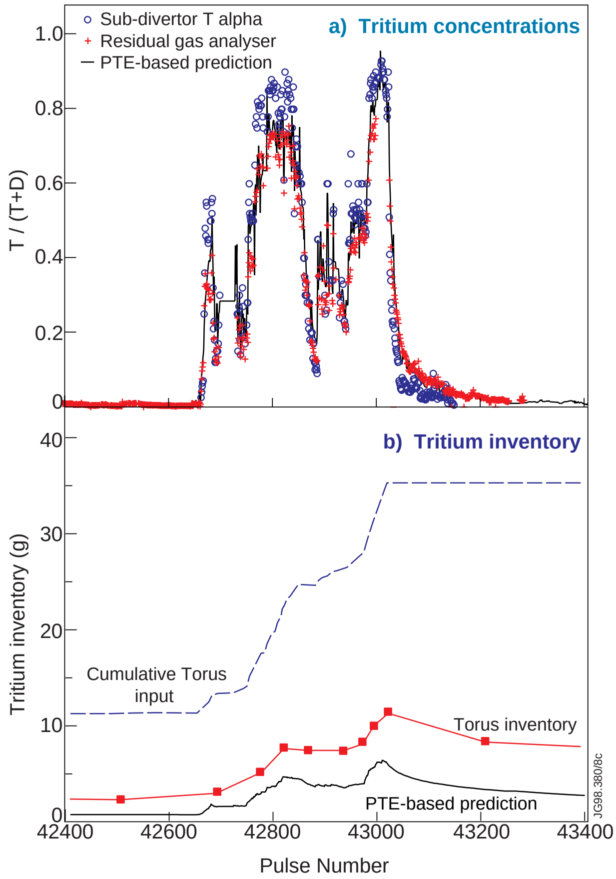

Fig. 1: (a) Tritium concentrations and (b) tritium inventory for the second period of DTE1 from September to November 1997 (Pulses No. 42661 to 43023).

In contrast, the tritium inventory (Fig. 1(b)) developed quite differently to the experience from the PTE: during the DTE1 campaign about 30% of the cumulative tritium input remained in the torus. This level was reduced to about 17% (~6 g) following extensive operation in hydrogen and deuterium; this was more than three times larger than had been expected from the tritium retention results of the PTE. This high level of tritium retention during and after DTE1 has been related to carbon films, saturated with deuterium and tritium and found in cold regions of the divertor [6]. While most of the JET vessel was heated to 320^{o}C, these cold regions, shadowed from direct contact with the plasma, were cooled to $\approx$ 50^{o}C (they act as a heat shield to protect the in-vessel divertor coils), allowing stable films to form with more than 40% hydrogen concentrations in carbon. (In contrast, at the time of the PTE, i.e. before the installation of a divertor, the whole vessel was maintained at 300^{o}C.) Extrapolation of these tritium retention results to ITER would result in unacceptably high tritium inventories, and the ITER divertor needs to be re-designed to take this fully into account.

3. STANDARD OPERATING MODE FOR ITER: STEADY-STATE ELMY H-MODE IN D-T

3.1. Mass scaling of H-mode threshold power

The effect of isotope mass on the heating power needed to access the H-mode regime (the H-mode threshold power) was studied during DTE1 in a series of experiments which included discharges with ≈60% and ≈90% tritium concentrations in deuterium. The most notable result was that, in comparison with previous experiments in pure deuterium, the H-mode threshold power was lower in D-T and lower still in pure tritium, roughly as the inverse of the atomic mass (A^{-1}). This can be seen in Fig. 2 which shows the loss power from the plasma plotted as a function of the scaling P_{Th}=0.76 $\bar{n}_e^{0.75}$B R^2 A^{-1}, which has been modified from that used for ITER [7] by the inclusion of an inverse mass dependence (the constant of proportionality has been adjusted to give the best fit to these JET data). Following DTE1, similar experiments were carried out in hydrogen, and these data are also shown in Fig. 2, and confirm the strong inverse mass dependence.

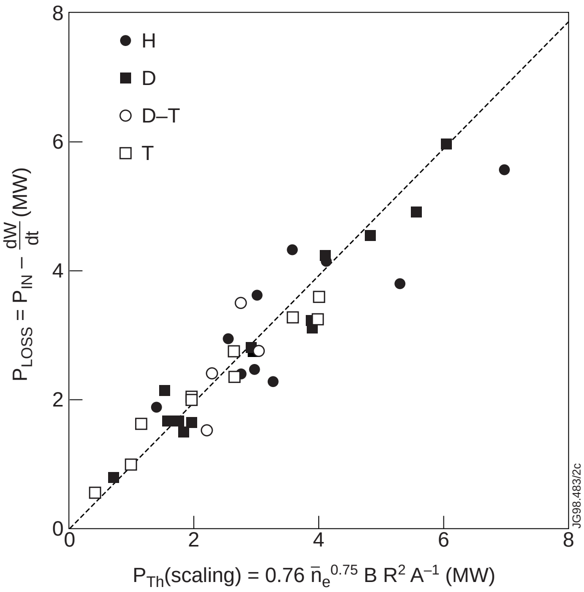

Fig. 2: Plasma loss power for ELMy H-mode discharges in hydrogen, deuterium, deuterium-tritium and tritium plotted against the ITER scaling for the H-mode threshold power modified to include an inverse mass dependence.

This result is very favourable for ITER since it predicts a 33% reduction in the power needed to access the H-mode in a pure tritium plasma (for example, during the start-up phase when it is important to achieve the high confinement of the H-mode as early as possible) and a 20% reduction in the H-mode threshold power for a 50:50 mixture of deuterium and tritium, thereby increasing the operational flexibility of ITER.

3.2. Mass dependence of energy confinement in ELMy H-modes

The most recent version of the multi-machine data base for steady state ELMy H-mode discharges shows that the global energy confinement time scales as $A^{0.2}$ with mass (the ITERH-EPS97(y) scaling [8] which is used at present for extrapolation to ITER). Before, during and after DTE1, steady state ELMy H-modes were obtained for a wide range of plasma currents (1-4.5 MA) and toroidal fields (1-3.8 T) in hydrogen, deuterium, D-T and tritium. The energy confinement times in these discharges were found to be consistent with the ITERH-EPS97(y) scaling, with its $A^{0.2}$ dependence providing an acceptable fit (Fig. 3). However, a more refined analysis shows that a better fit is with practically no mass dependence ($A^{0.03\pm0.1}$).

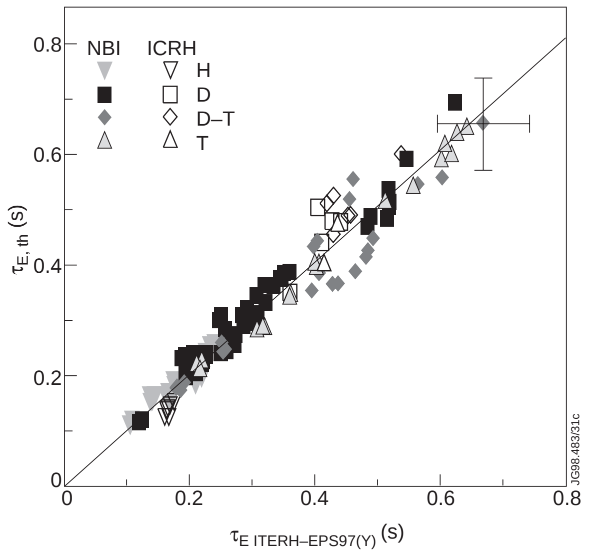

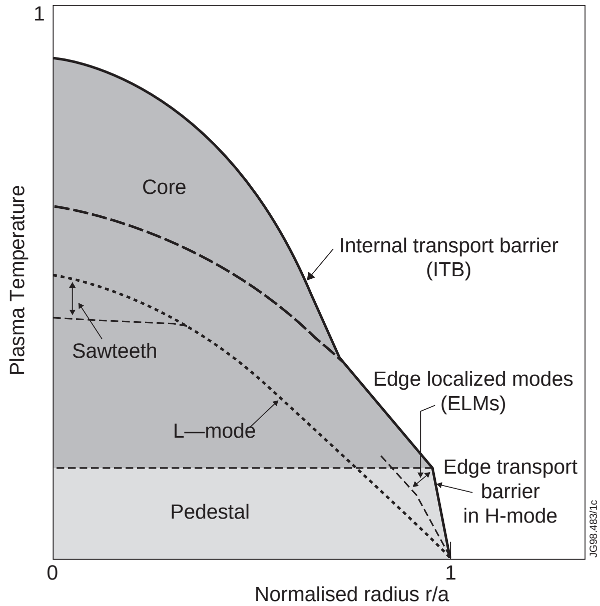

Fig. 3: Measured thermal energy confinement times in hydrogen, deuterium, deuterium-tritium and tritium ELMy H-mode discharges plotted against the ITER scaling law.

Fig. 4: Characteristic plasma temperature profiles in different modes of tokamak operation: L-mode, H-mode with edge transport barrier and optimised shear mode with internal transport barrier.

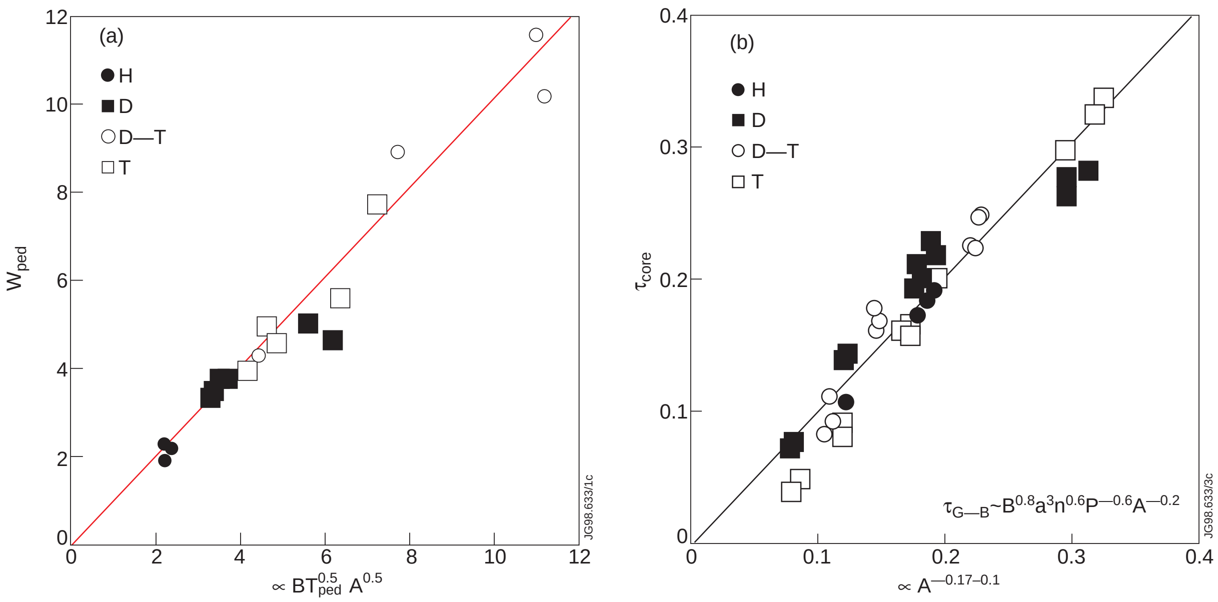

Fig. 5: (a) Pedestal energy plotted against that expected from an edge pressure gradient limited by ballooning modes over an ion poloidal Larmor radius and (b) thermal confinement time of the core plasma plotted against the best fit for the mass dependence in a pure gyro-Bohm scaling for ELMy H-mode discharges in hydrogen, deuterium, deuterium-tritium and tritium.

This result presents a challenge to theoretical understanding which may be resolved by separating the total stored plasma energy into two components (Fig. 4) which scale differently with respect to mass (and other significant parameters). The first component is the pedestal energy (Fig. 5(a)) which is determined from the edge temperature and density (assuming equal electron and ion temperatures at the plasma edge), and which shows a strong mass dependence.

The data shown is fitted by an $A^{0.5}$ dependence which would result, for example, from the gradient of the plasma pressure being limited in the edge by ideal ballooning mode instabilities over a distance characterised by the Larmor radius of ions [9]. The second component is the core energy which is determined by subtracting the pedestal energy from the total thermal plasma energy. The corresponding thermal core energy confinement time, $\tau_{core} = (W_{th}-W_{ped})/P$, is found to scale as $A^{-0.17\pm0.1}$ (Fig. 5(b)), consistent with the $A^{-0.2}$ mass dependence which would be expected from a gyro-Bohm scaling, generic of theoretical transport models based on turbulence with a scale length of the ion Larmor radius.

Differences between the edge and core transport is confirmed by local transport analysis using the TRANSP code. Figure 6 shows the ion thermal diffusivities as a function of normalised plasma radius for similar discharges in pure deuterium and in a 50:50 D-T mixture. It is clear from the figure that the mass dependence is different in the plasma core and edge, with the core data being consistent with gyro-Bohm scaling ($A^{0.5}T^{1.5}B^{-2}$). This means that energy transport in the plasma core can now for the first time be related to a theory-based scaling, including its mass dependence. It also emphasises that the large size of JET makes its data particularly valuable for separating core and edge effects in the global energy balance.

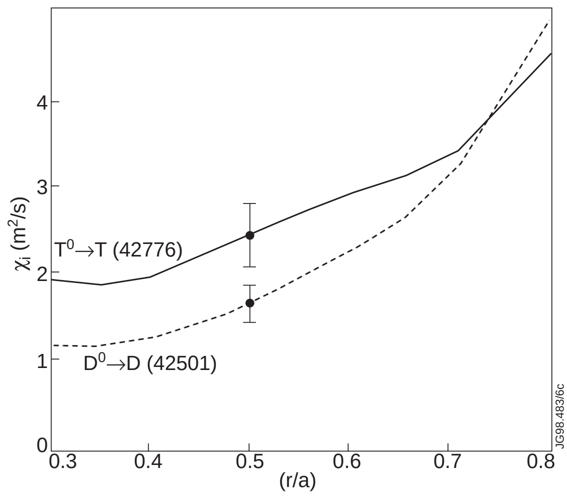

Fig. 6: Ion thermal diffusivities versus normalised plasma radius for ELMy H-mode discharges in deuterium and tritium.

3.3. ITER demonstration pulses in D-T

During DTE1 the best ever fusion performance in an ITER-like H-mode was obtained in a 3.8 MA/3.8 T discharge which was maintained in steady-state by regular Type I ELMs. This resulted in the production of a fusion energy of 21.7 MJ, a ratio of fusion power produced to input power of 0.18 over 3.5 s (≈8 energy confinement times) and 4 MW of fusion power being maintained for about 4 s.

The normalised plasma pressure, being limited to β_N=1.3 by the available additional heating power (23 MW of combined NB (90%) and ICRF (10%) heating), was too low for these discharges to qualify as ITER demonstration pulses. However, at lower toroidal field and plasma current (e.g. at 2 MA/2 T) the normalised plasma pressure (β_N=2.2) and collisionality of an ignited ITER were closely matched on JET and the edge safety factor was also close to the ITER value (q_{95}=3.2). The characteristic signals of such a discharge in D-T are shown in Fig. 7; it forms the basis for a series of “wind tunnel” experiments which preserve on JET all the relevant dimensionless parameters close to ITER values, except for the normalised plasma size, $\rho^*=\rho_i/a$.

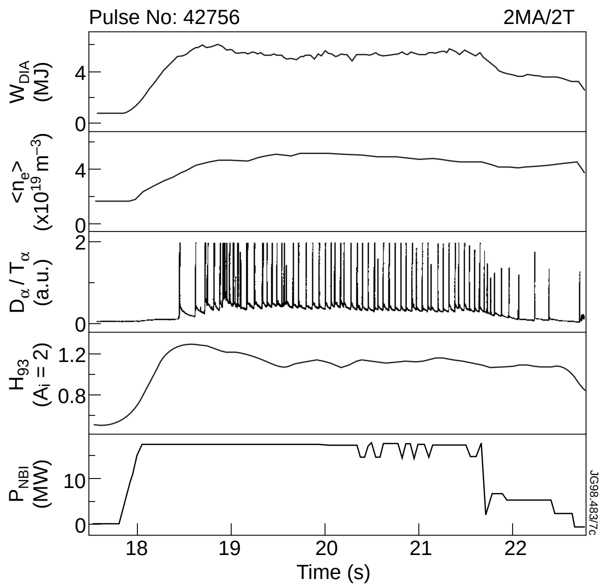

Fig. 7: Steady-state ELMy H-mode with ITER collisionality and normalised plasma pressure (β_N=2.4) in D-T. Such discharges formed the basis for "Wind Tunnel" experiments in JET.

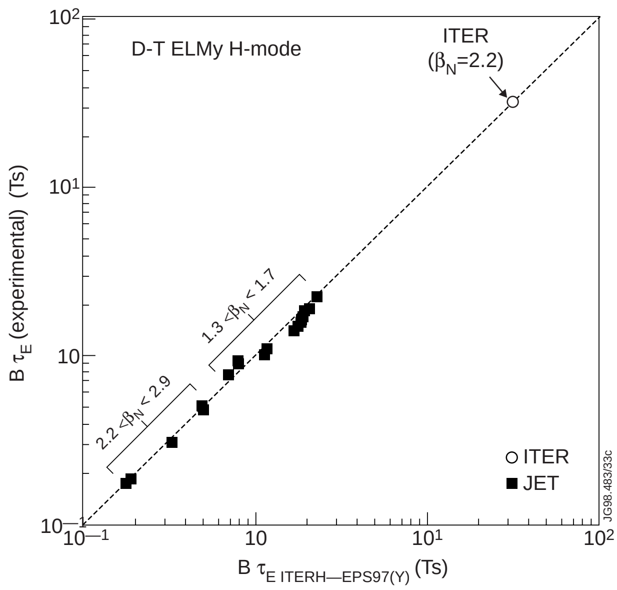

Fig. 8: Measured thermal energy confinement times of ITER similarity ELMy H-mode discharges in D-T plotted against the scaling law used in ITER projections. The operating point of an ignited standard ITER is also shown.

The data from this series of experiments is shown in Fig. 8 to scale close to gyro-Bohm, extrapolating to ignition in ITER. In fact, a gyro-Bohm extrapolation from these ITER demonstration pulses gives ignition at 1.8 GW (or Q=5.8 for a Bohm extrapolation) for ITER operating at 21 MA. The required density would, however, be 50% above the so-called Greenwald density limit, and confinement in JET and other tokamaks is degraded as this high density limit is approached (Fig. 9). During the 1998 campaign of JET experiments, the scaling of this density limit will be refined and the effect of deep fuelling using pellet injection rather than gas fuelling will be studied to determine any influence on confinement as higher densities are approached. Meanwhile, it has been possible to extend the ITER demonstration pulses to ITER operation at the higher plasma current of 24 MA (and correspondingly lower q_{95}=2.76). In this case, ignition is predicted at the 1 GW level for a gyro-Bohm extrapolation (or Q=7.3 for a Bohm extrapolation), but the required density is now lower and close to the Greenwald density.

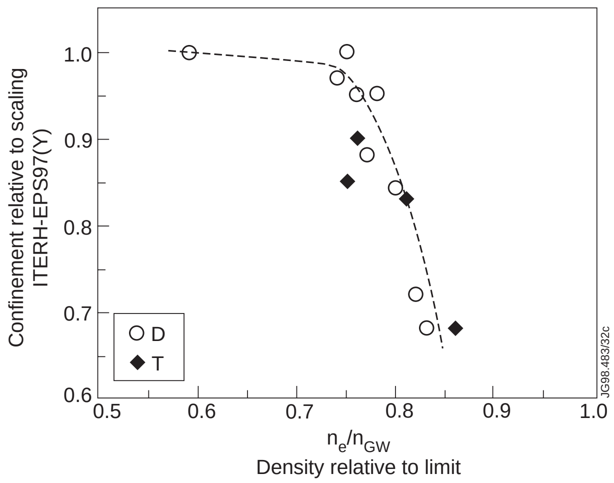

Fig. 9: Energy confinement time relative to the ITERH-EPS97(y) scaling versus density relative to Greenwald density. Confinement starts to degrade above 75% of Greenwald density.

4. ICRF HEATING OF D-T PLASMAS

Ion cyclotron resonance frequency (ICRF) heating is one of the main heating methods foreseen for ITER. During DTE1 the physics and performance of three ICRF schemes applicable to D-T operation ITER and a reactor were tested successfully [10].

4.1. Ion heating in deuterium and helium minority schemes

Deuterium minority heating, (D)T, at the fundamental resonance of deuterium (ω_{cD}) in tritium plasmas was demonstrated for the first time on JET [10]. The plasma density and the deuterium minority concentration (up to 20%) were optimised for maximum fusion power from reactions between suprathermal deuterons and thermal tritons. For a pulse with 9% deuterium and 91% tritium, an ICRH heating power of 6 MW generated 1.66 MW of fusion power and the fusion Q of this steady-state discharge was maintained at 0.22 for the length of the RF heating pulse (three energy confinement times) (Fig. 10). Doppler broadening of the neutron spectrum (Fig. 11(a)) showed a deuteron energy of 125 keV which was optimum for fusion reactions and close to the critical energy, resulting in strong bulk ion heating (T_{io}=7 keV at n_{eo}=5x10^{19} m^{-3}) and high fusion efficiency.

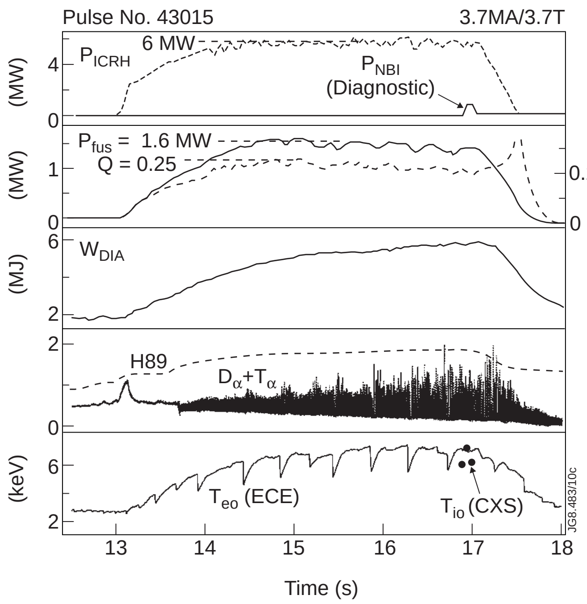

Fig. 10: H-mode plasma in which 6 MW of D(T) ICRF heating power gave 1.66 MW of fusion power resulting in a fusion gain of Q=0.22 in quasi steady-state.

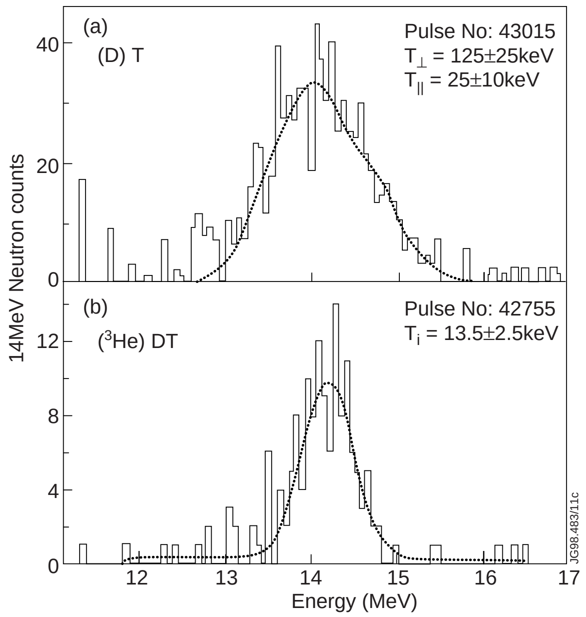

Fig. 11: Doppler broadened neutron spectra for discharges with (a) deuterium and (b) ^{3}He minority ICRF heating.

Helium minority heating, (^{3}He)DT, at the fundamental resonance of ^{3}He (ω_{c^3He}), in approximately 50:50 D:T plasmas with 5-10% ^{3}He, also produced strong bulk ion heating. As seen from the neutron spectrum of Fig. 11(b), the fusion reactions were thermal with central ion and electron temperatures of 13 and 12 keV, respectively. As discussed in Section 4.3, this scheme seems to be the most promising ICRF heating scheme for achieving ignition in ITER.

4.2. Electron heating in second harmonic tritium scheme

Heating at the second harmonic of tritium ($2\omega_{cT}$) in a 50:50 D:T plasma produced in JET energetic tritons well above the critical energy, resulting in mainly electron heating (≈ 90% of the power input). The fusion power was mainly from thermal reactions, but was typically a factor of four lower than with ^{3}He minority heating under similar conditions. Second harmonic tritium and fundamental ^{3}He minority ICRF heating are of course competing absorption mechanisms, since both resonances occur at the same position in the plasma.

The central ion and electron temperatures produced in these D-T experiments with the three ICRF heating methods are summarised in Fig. 12. The deuterium and ^{3}He minority schemes generated strong bulk ion heating and ion temperatures somewhat above the corresponding electron temperatures, whereas the second harmonic tritium ($2\omega_{cT}$)scheme heated mainly the electrons. Figure 11 also shows that the mean central temperature, $(T_{eo}+T_{io})/2$, with ($2\omega_{cT}$) heating was considerably lower than with the minority schemes. This is a consequence of the loss of energetic tritons (with energies > 5 MeV) in JET at moderate plasma currents.

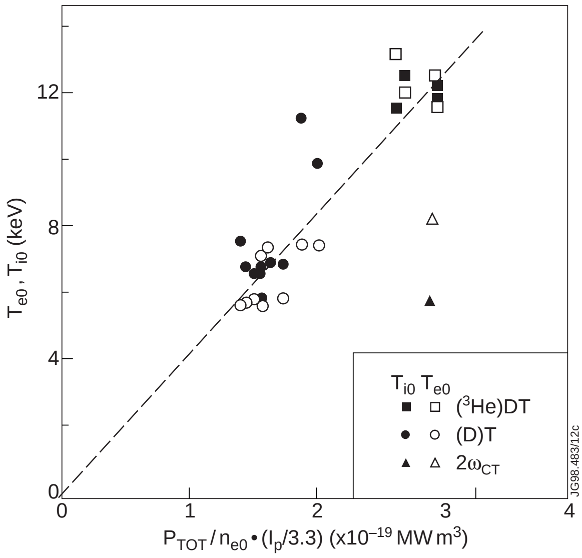

Fig. 12: Central ion and electron temperature plotted against power per particle, corrected for values of plasma current different to 3.3 MA.

4.3. Code calculations and predictions for ITER.

Most of the results obtained in these ICRF heating experiments are in excellent agreement with PION code predictions as exemplified by the comparison of measured and simulated neutron rates for a discharge with (D)T ICRF heating shown in Fig. 13. Such a high level of agreement gives confidence in the use of these models for predicting ICRF heating in ITER. One result of these predictions is that the $2\omega_{cT}$ scheme, which heats the electrons in JET, will give mainly ion heating in ITER where the power density per particle will be considerably lower, resulting in triton tail ions with lower energies. In addition, all fast ions will be confined in ITER, making heating at $2\omega_{cT}$ an efficient bulk ion heating scheme.

The PION code has also been used to investigate the ^{3}He minority scheme for ITER [11]. The results for a 2.5% concentration of ^{3}He in a 50:50 D:T plasma and a power of 50 MW are shown in Fig. 14 in the form of contour plots of constant ion heating fraction in the n_{eo}, T_{eo} space. For illustration a “direct” route from the ohmic (T_{eo}=5 keV, $n_{eo}=3.5x10^{19}$ m^{-3}) to the ignited phase (T_{eo}=35 keV, n_{eo}= $1x10^{20}$ m^{-3}) is shown for which the ion heating fraction is larger than 70%, making it an excellent heating scheme for ITER. As heating progresses, the ^{3}He concentration can be reduced further and the scenario changes to $2\omega_{cT}$ ion heating.

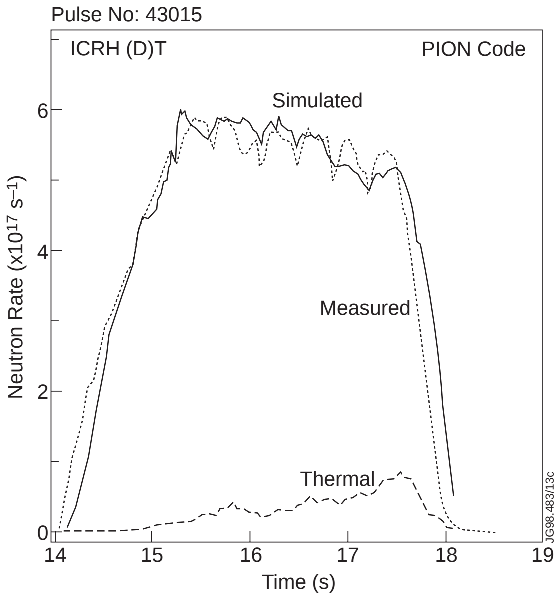

Fig. 13: Comparison of measured and simulated (with PION code) neutron rates for a discharge with deuterium minority ICRF heating showing excellent agreement between the two.

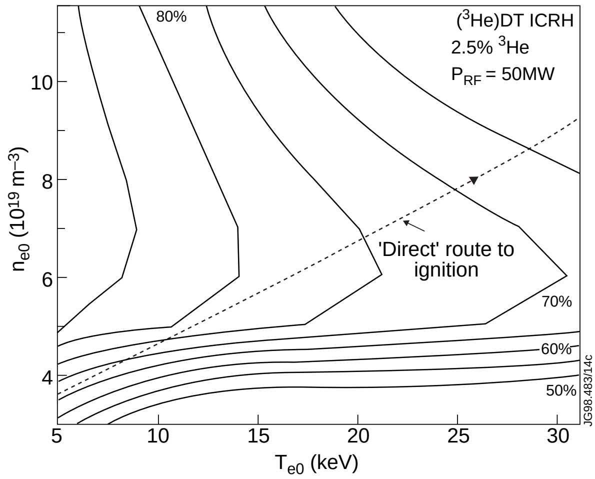

Fig. 14: Contours of constant bulk ion heating fraction for ITER parameters and 2.5% ^{3}He minority heating.

5. D-T FUSION PERFORMANCE AND RELATED PHYSICS

This section summarises the most important results of DTE1 in the areas of fusion performance, Alfvénic instabilities and alpha particle confinement and heating (for a more detailed discussion see [3]).

5.1. World records in fusion performance

In contrast to the steady-state ELMy H-mode discharge which produced a record fusion energy (see Section 3), the hot ion ELMy-free H-mode is the traditional mode of highest, but transient, performance [12] and, during DTE1, has led to records of fusion power and Q. In all, eight high power ELM-free H-mode pulses were produced in D-T, five of which delivered more than 12 MW of fusion power. Fig. 15 shows the pulse with the highest fusion power of 16.1 MW (a similar pulse on the same day, about one hour earlier, produced 15.8 MW), which was obtained with 25.4 MW of additional heating using 22.3 MW of NB heating together with 3.1 MW of hydrogen minority ICRF heating. In common with the ELM-free H-mode discharges in deuterium, the stored energy (not shown), fusion power and electron density (not shown) rise monotonically with time. The ion temperature levels off around 28 keV, significantly higher than the electron temperature which is about 14 keV. The ELM-free period is limited by MHD activity(as seen in the structure of the Balmer alpha signal): first an outer mode and then a giant

ELM [13]. Following detection of the giant ELM, the heating power is switched off to save neutrons. As shown in the lowest panel of Fig. 15, this pulse reaches a record fusion gain $Q_{in} = P_{fus}/P_{in}$=0.62 and a ratio of fusion power to total loss power $Q_{tot} = P_{fus}/(P_{loss}-P_{\alpha})$ = 0.95±0.17, the value which Q_{in} would reach if a similar plasma could be obtained in steady-state. The value of Q_{tot}=0.95 is in line with expectations based on the value of the fusion triple product $n_{DT}(o)\tau_E T_i(o)$ of 8.7x10^{20} m^{-3} s keV ± 20%.

In addition, a thorough comparison of similar D-T and D-D discharges in JET has validated the factor of 210 between D-D and D-T fusion power expected from the respective reaction rate coefficients [14]. This is a very important confirmation that the expected fusion performance can be achieved in D-T plasmas.

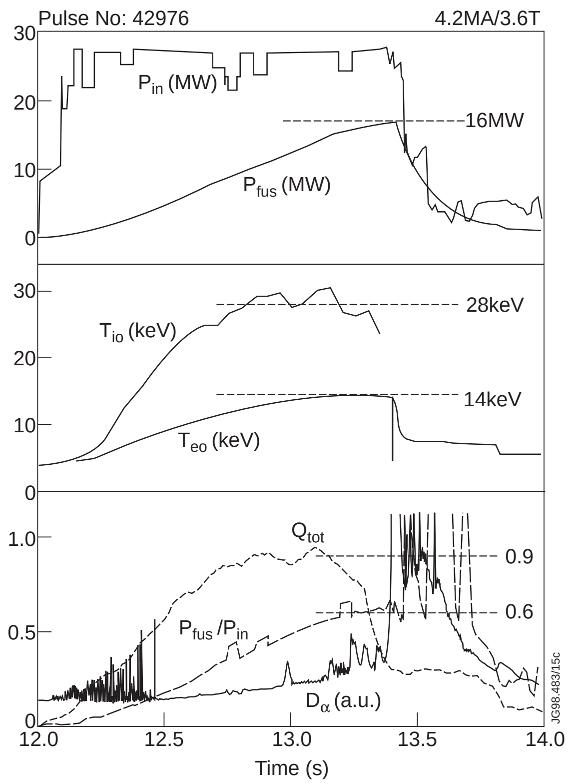

Fig. 15: Various time traces for the highest fusion yield hot-ion H-mode discharge. From top to bottom: Input and fusion power; central ion and electron temperatures; ratios of fusion to input power, Q_{in}, and of fusion to loss power, Q_{tot}, and D_α/T_α intensity.

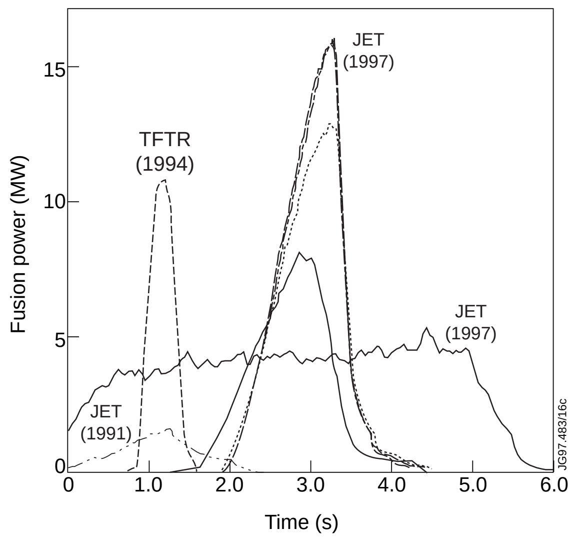

Fig. 16: Fusion power development in JET (1991 and 1997) and TFTR (1994).

Figure 16 summarises the development of fusion power over the last six years in JET and TFTR. It encompasses the first ever high fusion power (1.7 MW) pulse with 11% tritium in JET in 1991 [1], the pulse with the highest fusion power (10.7 MW) [15] from the 50:50 D-T experiments on TFTR during the period 1993 to 1997, and finally the record pulses from the JET D-T experiments in 1997 [2,3]: 16.1 MW, transiently, in an ELM-free H-mode, 8.2 MW in the optimised shear mode of operation (see Section 6), and 4 MW in a steady-state ELMy H-mode discharge.

5.2. Alpha particle driven Alfvénic instabilities

Fast particles involved in plasma heating (eg. fast ions from ICRF heating or NB heating, alpha particles) can resonate with Alfvén waves, leading to particle and energy losses and possible destructive interaction with vessel components. An important question in relation to high performance fusion plasmas is therefore whether the alpha particles, while slowing down from their birth energy of 3.5 MeV, induce Alfvénic instabilities.

As can be seen from Fig.17(b) no alpha particle driven Toroidal Alfvén Eigenmodes (TAEs) were excited in the record fusion power D-T discharges, even though TAEs have been observed under other circumstances in JET, eg. hydrogen minority ICRF heating in deuterium plasmas above an RF power of 5 MW [16], as seen from the magnetic fluctuation spectra shown in Fig. 17(a). The absence of alpha particle driven instabilities in these high performance discharges is in agreement with stability calculations which show that the normalised alpha particle pressure in these discharges is a factor of two below the instability threshold [17].

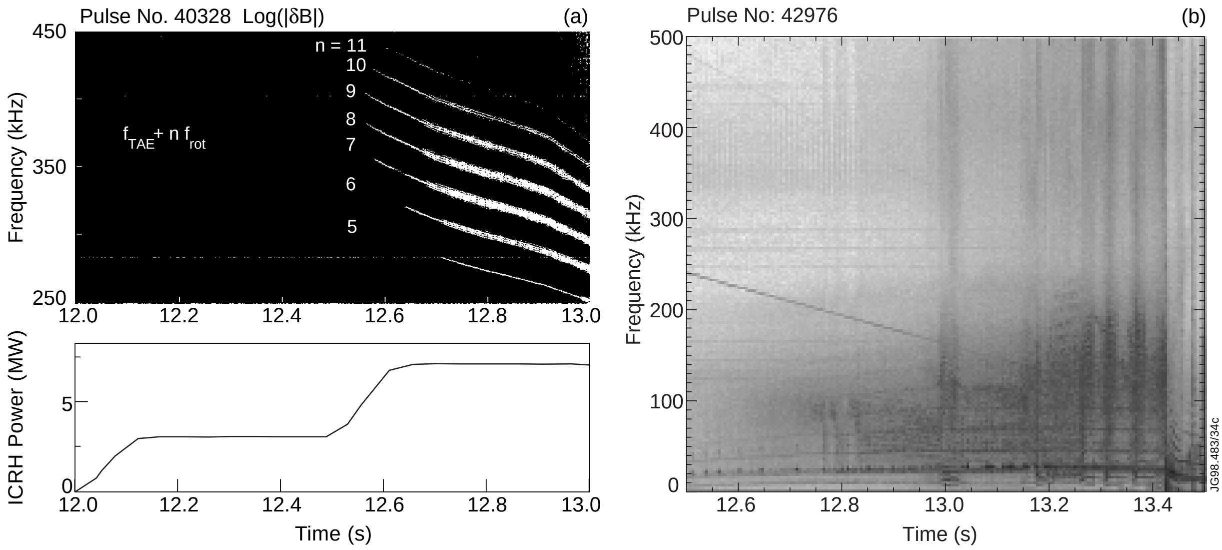

Fig. 17: Magnetic fluctuation spectra showing (a) clear TAE activity above 5 MW of hydrogen minority ICRF heating but (b) no alpha particle driven TAEs in record fusion power discharge in D-T.

5.3. Alpha particle confinement and heating

One of the most important objectives of the JET high performance D-T experiments was an unambiguous demonstration of alpha particle heating, thus confirming the process by which ignition and self-sustained burn would occur in ITER and a reactor. Since JET plasmas with the highest fusion performance have about 3 MW of alpha particle heating compared to a total input power of about 25 MW, and the alpha particle heating is centrally peaked and couples mainly to the electrons, it should be observable, despite competition from other inputs to the electrons.

To separate the alpha particle heating from possible isotope effects on energy confinement, a series of specially designed pulses was carried out in which the D-T mixture was varied from pure deuterium to almost pure tritium while all other parameters including the external heating power (≈10.5 MW NB heating) were kept as constant as possible [18]. Comparing the pure deuterium and almost pure tritium ends of this scan demonstrated (lower panel in Fig.18) that the global energy confinement time in ELM-free H-modes has no or only a very weak isotope dependence. The slight increase in confinement in the centre of the scan is due to the peaked alpha power source which nearly doubled the power transferred to the electrons in the centre. The strong correlation between the maximum diamagnetic and thermal plasma energies and the optimum D-T mixture (upper panel in Fig. 18), is a clear demonstration of alpha particle heating. This is seen even more clearly in Fig. 19, where the central electron temperature is plotted versus the calculated alpha particle heating power for the set of pulses in the D-T mixture scan. The highest electron temperature shows a clear correlation with the maximum alpha particle heating power and with the optimum D-T plasma mixture (40:60). A regression fit to the data gives a change in central electron temperature of 1.3±0.23 keV with 1.3 MW of alpha particle heating power.

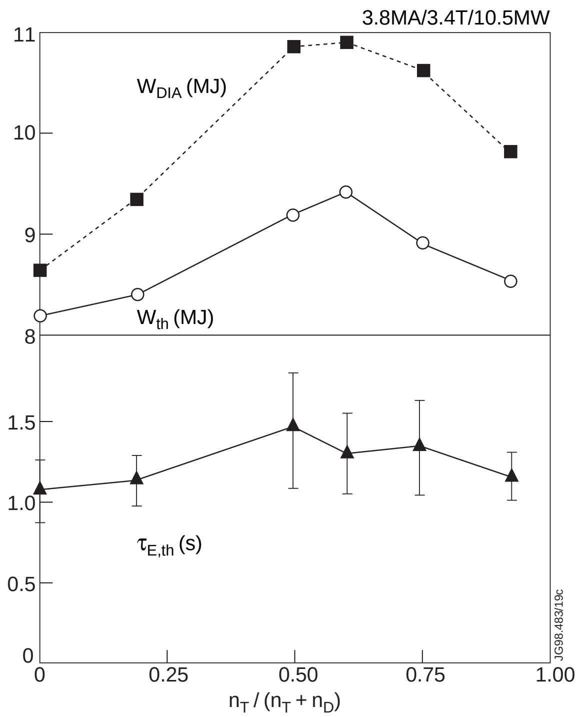

Fig. 18: Diamagnetic and thermal plasma energy contents (top) and global energy confinement time (bottom) versus tritium concentrations.

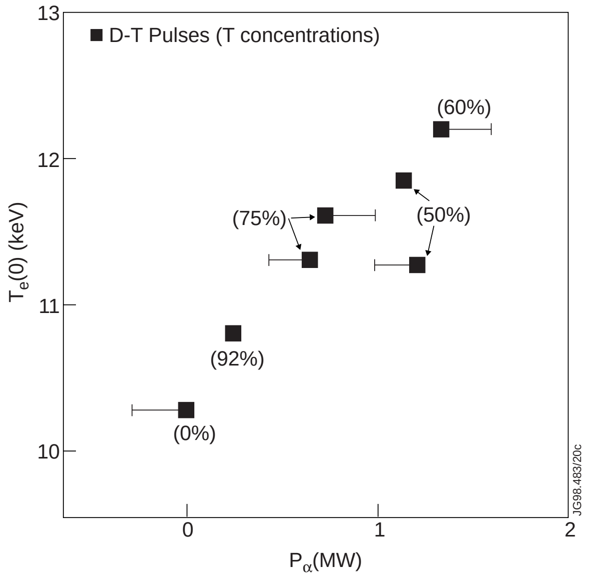

Fig. 19: Central electron temperature versus alpha particle heating power. The bars indicate the variation in NB power compared to the 92% tritium reference pulse. The figures in brackets are the tritium concentrations.

These JET experiments are a clear demonstration of the self-heating of a D-T plasma by the alpha particles produced by fusion reactions. A comparison with ICRF heating of deuterium plasmas under similar conditions showed that the alpha particle heating was as effective as hydrogen minority ICRF heating (which, like the alpha particles, mainly heats the electrons).

This is a strong indication that, in the absence of alpha particle driven TAE instabilities (see Section 5.2), the trapping and slowing down of the alpha particles and their heating effect are classical and that there are no unexpected effects which might prevent ignition in a larger device.

6. ADVANCED OPERATING MODE FOR ITER: OPTIMISED SHEAR MODE IN D-T

The advanced tokamak concept proposes the use of profile control techniques to engineer high plasma confinement and to develop these conditions into steady-state. This concept, if successful, would give ignition and sustained burn at lower plasma current, thereby reducing the size and cost of a reactor. JET has been particularly suited to such studies by virtue of its combination of heating schemes and its current drive capability. In fact, JET reported the first observations of such plasma behaviour in the Pellet-Enhanced Performance (PEP)-mode of 1988 [19, 20]. More recently, JET developed a particular optimised shear scenario in which pressure profiles are more peaked and D-D neutron yields are higher than in the ELM-free H-mode [21, 22].

6.1. Formation of internal transport barriers

A key element in these scenarios [21-25] is the formation of an internal transport barrier (ITB) and these have now been established for the first time in D-T [26]. Power and current profile control are used to establish an ITB, to delay the transition to an H-mode phase, and to avoid a β limit disruption [21, 22]. The scenario comprises the formation of a target plasma by pre-heating during a fast current ramp, using lower hybrid waves to assist breakdown and to provide some current drive, followed by ICRF pre-heating to slow current penetration. When the current profile is such that the volume within the q=2 surface is reasonably large (r/a≈0.3-0.4), the full heating power, typically 16-18 MW of NB heating together with 6 MW of ICRF heating, is applied (Fig. 20). In D-D the highest fusion performance has been obtained when a clear H-mode transition was delayed for as long as possible by using low target density, strong divertor

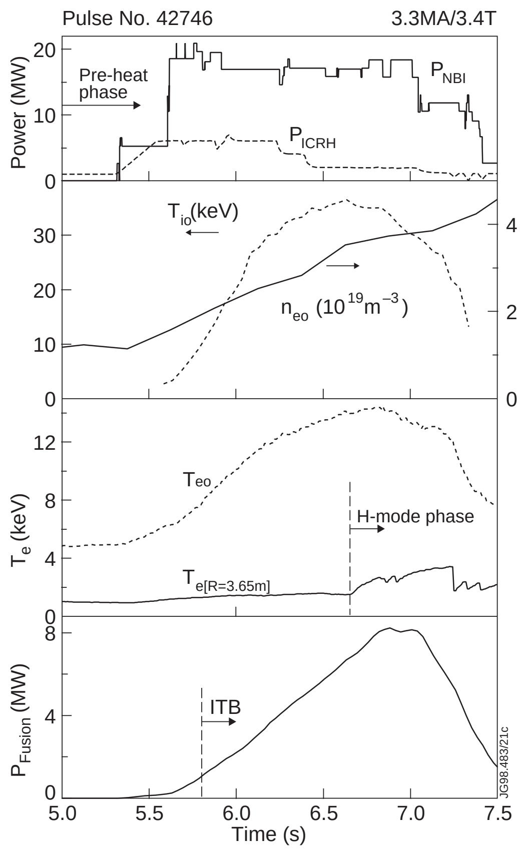

Fig. 20: Various time traces for the optimised shear discharge with the highest fusion yield. From top to bottom: NB and ICRF input power; central ion temperature and electron density; central and edge (R=3.65m) electron temperature; and fusion power.

pumping and low triangularity and by maintaining the current ramp throughout the main heating phase. When an ITB is established, the resulting good core confinement maintains the plasma loss power below the level required to trigger an H-mode, thus preserving an L-mode edge.

In D-T plasmas, the scenario had to be modified, largely because of the lower H-mode threshold power [9, 4]. However, after some scenario development, strong ITBs were established for the first time in D-T plasmas, and with a threshold heating power and current profiles not markedly different from those in D-D [26]. In D-T, as in D-D, the foot of the steep gradient region was located just inside the q=2 surface and both moved outwards with time.

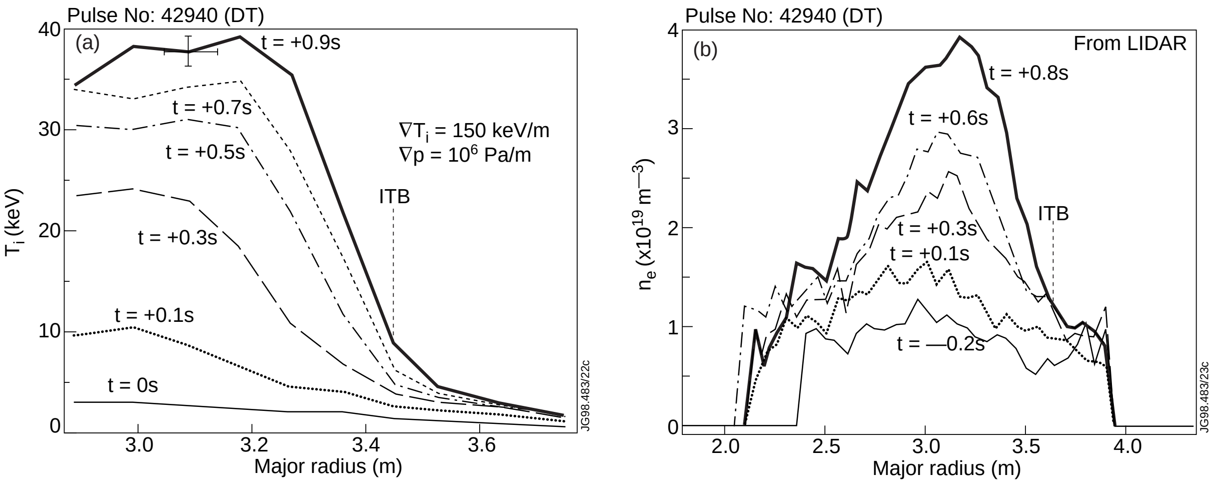

Fig. 21: (a) Ion temperature and (b) electron density profiles at various times after the start of high power heating in an optimised shear discharge showing the formation of an internal transport barrier (ITB).

When an ITB forms, substantial increases in plasma density and temperature occur during the first second of high power heating (Fig. 21). As shown in Fig. 21(a), the temperature gradient can reach 150 keV/m and the pressure gradient 1 MPa/m. The input power is controlled by feedback on the neutron rate in order to avoid excessive pressure gradients which provoke MHD instabilities. As a result, the plasma can be maintained close to the ideal MHD stability limits [27] for most of the heating pulse, as shown in Fig. 22 for optimised shear discharges in D-D and in D-T. In both cases, β_N increases as the ITB moves outwards with time to about 2/3 of the plasma radius and the pressure profile becomes less peaked. Towards the end of the discharge, an H-mode forms, reducing further the peaking and moving the discharge away from the instability boundary but also leading to the subsequent termination of the discharge by disruption. The highest performance has been achieved with small or slightly reversed central shear and q(0) in the range 1.5-2.

This is confirmed by TRANSP simulations, which also show that more than half of the full plasma current at peak performance was driven non-inductively, with the bootstrap and NB driven currents being about equal and localised close to the centre. Furthermore, the TRANSP

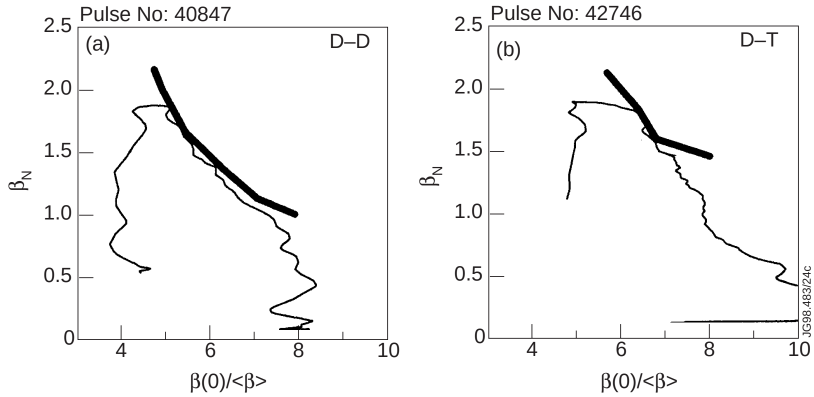

Fig. 22: Evolution of normalised plasma pressure and stability boundary for two optimised shear discharges, (a) one in D-D and (b) one in D-T.

calculations show [26] that the ion thermal diffusivity can be very low and close to neoclassical [28] values within the ITB (Fig. 23).

The neutron and time constraints on DTE1 did not allow these discharges to be optimised. Nevertheless, 8.2 MW of fusion power was produced (Fig. 20), even though the tritium concentration (≈30%) and central density ($4x10^{19}m^{-3}$) were relatively low and the ion temperature (≈40 keV) was too high for maximum fusion reactions.

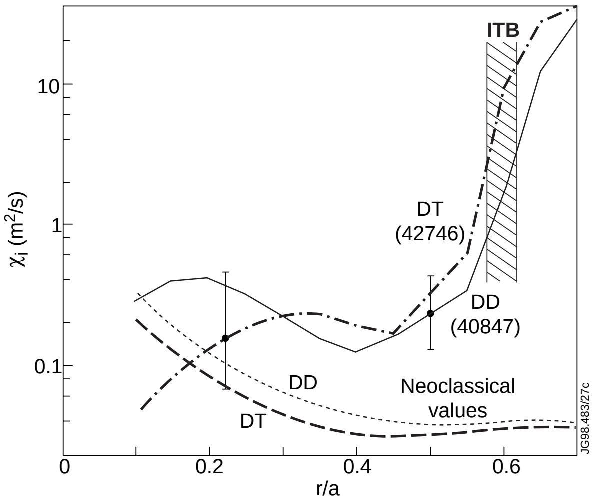

Fig. 23: Ion thermal diffusivities versus normalised plasma radius for two optimised shear discharges in D-D and D-T and comparison with neoclassical values.

6.2. Simultaneous internal and edge transport barriers and development towards steady-state

The highest fusion performance was normally obtained by prolonging the phase during which the plasma edge was L-mode [21, 22]. A significant number of discharges, however, developed both an ITB and an ELMy H-mode edge [3] as illustrated in Fig. 24, and still produced a substantial fusion yield. In the discharge shown in Fig. 24, an ITB is formed and the central ion temperature reaches 24 keV, while the edge ion temperature is about 3 keV, typical of an ELMy H-mode.

In this pulse the fusion power increases from the start of the main heating phase until it reaches 6.8 MW, at which time the input power was reduced to economise on D-T neutrons. This increase in fusion yield is due to a continuous build-up of central density together with an increase of the tritium concentration. The stored plasma energy reaches 8.8 MJ for a total input power of 18.4 MW and a corresponding confinement enhancement factor H_{89}≈2.3 relative to the ITER89-P scaling [29]. In this pulse, as in similar D-T and D-D pulses, the positions of the

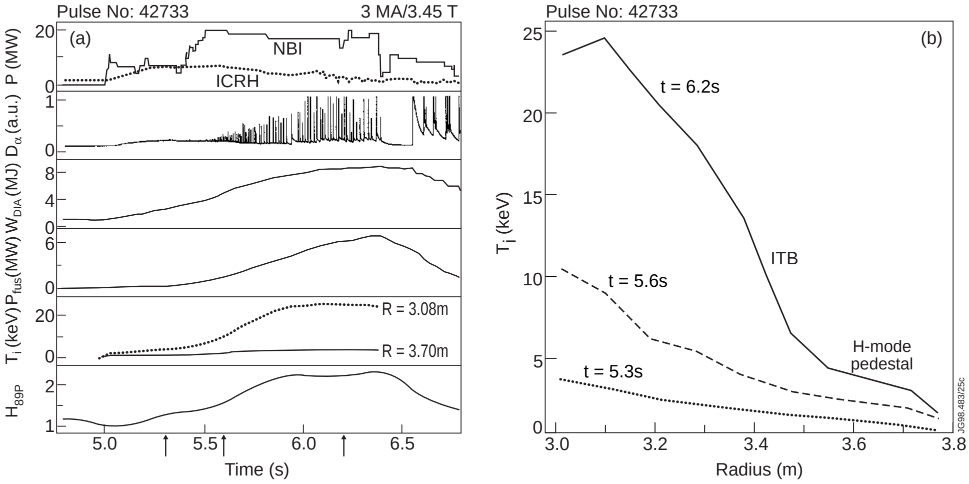

Fig. 24: (a) Various time traces and (b) ion temperature profiles for a pulse which develops an internal transport barrier simultaneously with an ELMy H-mode barrier.

q=2 magnetic surface and the ITB change only slowly with time. This can be interpreted as a consequence of the generation of an edge bootstrap current. At 6.4 s, the input power was stepped down to limit the number of D-T neutrons produced; the subsequent collapse of the ITB triggers an ELM-free H-mode.

A comparison of the double barrier (ITB plus ELMy H-mode) discharge shown in Fig. 24 with a conventional ELMy H-mode discharge without an ITB in the same plasma configuration and with similar input power (22.5 MW) shows the advantage of the double barrier plasma: the fusion triple product $n_i(o)T_i(o)\tau_E$ reaches 4.4 x $10^{20}m^{-3}$ keVs compared to 1.9 x $10^{20}m^{-3}$ keVs and the fusion Q is 0.4 compared to 0.2 [30]. In addition, ELMs are of much smaller amplitude in double barrier discharges which is of great significance because of the critically high peak power loads on the divertor target plates in a standard ELMy H-mode ignited ITER scenario.

This route, which could not be explored further during DTE1 because of the imposed constraint on the number of D-T neutrons produced, shows significant promise for steady-state high fusion yield D-T plasmas, but would require a technique for better control of the plasma edge and/or the current profile.

6.3. Projections to future JET operations

As indicated in Section 6.1, it was not possible to optimise the fusion performance of the optimised shear discharges during DTE1 due to the imposed constraint on neutron budget. Some code calculations were run, however, to determine what might be expected in future D-T operations on JET. These time dependent transport code and MHD stability calculations which have been calibrated against existing optimised shear discharges in JET and Tore Supra show that significant performance improvements are possible in JET [31]. The performance projections, in which the thermal fusion power is scaled from existing pulses as β_N^2 and the non-thermal fusion power is scaled proportional to the NB heating power, predict for operation with a magnetic field of 4 T a fusion power of ≈30 MW and a fusion gain $Q_{in} = P_{fus}/P_{in} \geq 1$ with the existing heating and current drive systems, and even higher performance with modest upgrades.

7. SUMMARY AND CONCLUSIONS

The recent D-T and ITER physics campaigns on JET have produced a wealth of unique and pertinent physics results, improving our theoretical understanding and allowing more accurate predictions for ITER:

- The standard ITER operating mode (steady-state ELMy H-mode) has been well characterised empirically and a theoretical basis for energy confinement in the plasma core is within reach. The results of the dimensionless scaling "Wind Tunnel" experiments extrapolate to ignition with standard ITER parameters.
- Radio frequency heating of D-T plasmas is well understood and most effects are well simulated by theory. The results predict efficient bulk ion heating on the way to ignition in ITER.
- Alpha particle heating was clearly observed and is consistent with classical expectations, thus confirming the process by which ignition would occur in ITER and a reactor.
- The advanced ITER operating mode (optimised shear) takes confinement to the most favourable theoretical expectations (i.e. ion heat conduction reaches neoclassical values) and the plasma pressure is limited in accord with theory. This improves the basis for performance optimisation (high plasma pressure, long pulse) by profile control which will be persued in JET operations in 1998/99.

With its unique combination of divertor configuration, heating and profile control systems and tritium capability, JET will remain, for many more years, the most valuable machine in support of ITER or any other Next Step tokamak.

ACKNOWLEDGEMENTS

The author wishes to thank all his colleagues at JET who have made these significant achievements possible and in particular M L Watkins, J G Cordey, C Gormezano, P J Lomas, F X Söldner, D F Start and P R Thomas for their contributions to this paper and B E Keen for his help with the editing.

REFERENCES

[1] JET Team, Nucl. Fusion **32** (1992) 187.

[2] GIBSON, A., and the JET Team, Physics of Plasmas **5** (1998) 1839.

[3] KEILHACKER, M. et al., and the JET Team, "High Fusion Performance from Deuterium-Tritium Plasmas in the JET Tokamak", accepted for publication in Nucl. Fusion (1999).

[4] JACQUINOT, J. et al., and the JET Team, "Overview of ITER Physics Deuterium-Tritium Experiments in JET", accepted for publication in Nucl. Fusion (1999).

[5] AYMAR, R., CHUYANOV, V., HUGUET, M., PARKER, R., SHIMOMURA, Y. and the ITER Joint Central Team and Home Teams, in Fusion Energy 1996 (Proc. 16th Int. Conf. Montreal, Canada, 1996) Vol. 1, IAEA, Vienna (1997) 3.
[6] ANDREW, P.L. et al., 13th Conf. on Plasma Surface Interactions in Controlled Fusion Devices, San Diego, USA, 1998, to be published in J. Nucl. Materials (1999).
[7] ITER Confinement Database and Modelling Expert Group (presented by T. Takizuka), in Fusion Energy 1996 (Proc. 16th Int. Conf. Montreal, Canada, 1996) Vol. 2, IAEA, Vienna (1997) 795.
[8] ITER Confinement Database and Modelling Working Group, presented by J.G. Cordey, Plasma Phys. Control. Fusion **39** (1997) B115.
[9] The JET Team (presented by M. Keilhacker), Plasma Phys. Control. Fusion **39** (1997) B1.
[10] START, D. F. H. et al., Phys. Rev. Lett. **80** (1998) 4681.
[11] START, D. F. H. et al., in Europhysics Conference Abstracts (Proc. 24th EPS Conference on Controlled Fusion and Plasma Physics, Berchtesgaden, Germany, 1997), Vol 21A, Part 1, 141.
[12] JET Team (presented by P. J. LOMAS), in Fusion Energy 1996 (Proc. 16th Int. Conf. Montreal, Canada, 1996) Vol. 1, IAEA, Vienna (1997) 239.
[13] NAVE, M. F. F. et al., Nucl. Fusion **37** (1997) 809.
[14] MARCUS, F. B. et al., Nucl. Fusion **33** (1993) 1325.
[15] McGUIRE, K. M. et al., in Fusion Energy 1996 (Proc. 16th Int. Conf. Montreal, Canada, 1996) Vol. 1, IAEA, Vienna (1997) 19.
[16] FASOLI, A. et al., Plasma Phys. Control. Fusion **39 (**1997) B287.
[17] SHARAPOV, S. E. et al., “Stability of Alpha Particle Driven Alfvén Eigenmodes in High Performance JET D-T Plasmas” accepted for publication in Nucl. Fusion (1999).
[18] THOMAS, P. R. et al., Phys. Rev. Lett. **80** (1998) 5548.
[19] The JET Team (presented by J. Jacquinot), Plasma Phys. Control. Fusion **30** (1988) 1467.
[20] HUGON, M. et al., Nucl. Fusion **32** (1992) 33.
[21] JET Team (presented by C. GORMEZANO), in Fusion Energy 1996 (Proc. 16th Int. Conf. Montreal, Canada, 1996) Vol.1, IAEA, Vienna (1997) 487.
[22] JET Team (presented by F. X. SÖLDNER), Plasma Phys. Control. Fusion **39** (1997) B353.
[23] KESSEL, C. et al., Phys. Rev. Lett. **72** (1994) 1212.
[24] STRAIT, E. J. et al., Phys. Rev. Lett. **75** (1995) 4421.
[25] USHIGUSA, K., and the JT-60 Team, in Fusion Energy 1996 (Proc. 16th Int. Conf. Montreal, Canada, 1996) Vol.1, IAEA, Vienna (1997) 37.
[26] GORMEZANO, C., et al., Phys. Rev. Lett. **80** (1998) 5544.
[27] HUYSMANS, G. T. A. et al., 24th Europ. Phys. Soc. Conf. on Controlled Fusion and Plasma Physics Berchtesgaden, Germany (1997) Vol. 21A, Part 1, 21.

[28] HINTON, F.L. and HAZELTINE, R.D., Reviews of Modern Physics **48** (1976) 239.
[29] SCHISSEL, D.P. et at., Nucl. Fusion **31** (1991) 73.
[30] SÖLDNER, F.X. et al., “Approach to Steady-State High Performance in DD and DT with Optimised Shear in JET”, accepted for publication in Nucl. Fusion (1999).
[31] KEILHACKER, M., WATKINS, M.L. and the JET Team, Proceedings of the 13th Conference on Plasma Surface Interactions in Controlled Fusion Devices, San Diego, USA, 1998, Invited Paper, to be published in J. Nucl. Materials (1999).